ELSEVIER

Chemical Engineering Journal 135 (2008) 103–112

Chemical Engineering Journal

www.elsevier.com/locate/cej

Discrete particle simulation of particle flow in IsaMill—Effect of grinding medium properties

C.T. Jayasundara [a], R.Y. Yang [a], A.B. Yu [a,*], D. Curry [b]

[a] *Centre for Simulation and Modelling of Particulate Systems, School of Materials Science and Engineering, The University of New South Wales, Sydney, NSW 2052, Australia*

[b] *Xstrata Technology, Brisbane, Qld 4000, Australia*

Received 31 July 2006; received in revised form 22 March 2007; accepted 1 April 2007

Abstract

Simulations based on discrete element method (DEM) were conducted to investigate the effect of particle properties, such as particle/particle sliding friction, particle/particle restitution coefficient, particle density and particle size, on the particle flow in IsaMill. The results were analysed in terms of velocity distribution, porosity distribution, collision frequency, collision energy and power draw. It is shown that by decreasing particle/particle sliding friction coefficient, the flow of particles becomes more vigorous which is useful to grinding performance. Although restitution coefficient does not significantly affect the particle flow in IsaMill, grinding media with higher restitution coefficient should be more effective for grinding because they often have higher collision frequency and collision energy. Heavier particles tend to have higher collision frequency and collision energy but require higher power input, so there may exist an optimum particle density for maximum process efficiency. Grinding medium size also affects the flow and hence grinding behaviour although its selection may mainly depend on the particle size of products. The results obtained from the DEM model should be useful for the selection of grinding media for IsaMill process.

Keywords: Grinding; Milling; Discrete element method; Granular dynamics

1. Introduction

IsaMill is a high-speed stirred mill developed by Mount Isa Mines (Xstrata) in Australia for fine and ultra fine grinding at an industrial scale [1]. Comparing with the conventional grinding mills such as ball mills and tower mills, IsaMill can significantly reduce comminution circuit energy cost and grind mineral particles to as fine as 7 μm [2,3]. As a result, it can be applied to base metal operations such as lead and zinc mines, and also for the liberation of gold particles from sulphide minerals for cyanidation. Furthermore, its ability to use cheaper non-metallic grinding media (river sand, furnace slag, etc.) offers further process and cost benefits over traditional grinding technologies.

IsaMill, however, is still a new technology and at present, its optimum control and scale-up mainly rely on empirical methods, experience and trial and error tests. Fundamental understanding of the grinding mechanism and flow pattern in the mill is essential for process control and reliable scale-up. Conventional experimental techniques and numerical models developed within a continuum framework (e.g. CFD) [4] mainly focus on the phenomena at a macroscopic level and cannot obtain information at a microscopic, particle level. This limitation can be effectively overcome by the numerical model based on the discrete element method (DEM) [5], which describes the motion of particles individually. The method has been used to study different milling processes [6–11], and more recently has been applied to simulate a simplified IsaMill consisting of one or three discs [12–14]. The microdynamic properties relating to flow and force structures were analysed and the effects of the mill properties and operational conditions on these properties were investigated.

The flow in IsaMill is also affected by particle properties. For example alloy steel balls, due to their high relative density and hardness, are particularly suitable for crushing and mixing heavy, hard materials. The forged steel balls, on the other hand, are used to reduce particle size and fine dispersion of highly viscous fluids [15]. The dispersity is characterized by particle size distribution, particle shape and morphology, and their interfacial

* Corresponding author. Tel.: +61 2 9385 4429; fax: +61 2 9385 5969.
E-mail address: a.yu@unsw.edu.au (A.B. Yu).

1385-8947/$ – see front matter © 2007 Elsevier B.V. All rights reserved.
doi:10.1016/j.cej.2007.04.001

properties which are related to sliding friction coefficient, mass density and restitution coefficient [16]. However, quantification of the effects of some material variables by physical experiments is difficult. The objective of this study is to extend our previous DEM work to investigate the effects of grinding medium properties, such as particle/particle sliding friction, particle restitution coefficient, particle density and particle size on the particle flow in IsaMill.

2. Simulation method

In DEM simulation, each particle possesses translational and rotational motion, which can be described by Newton's second law of motion, given by

$$m_i \frac{\mathrm{d}\mathbf{v}_i}{\mathrm{d}t} = \sum(\mathbf{F}_{ij}^{\mathrm{n}} + \mathbf{F}_{ij}^{\mathrm{s}} + m_i\mathbf{g}) \quad (1)$$

and

$$I_i \frac{\mathrm{d}\boldsymbol{\omega}_i}{\mathrm{d}t} = \sum(\mathbf{R}_i \times \mathbf{F}_{ij}^{\mathrm{s}} - \mu_{\mathrm{r}} R_i |\mathbf{F}_{ij}^{\mathrm{n}}| \boldsymbol{\omega}_i) \quad (2)$$

where m_i, $\mathbf{v}_i$, $\boldsymbol{\omega}_i$ and I_i are, respectively, the mass translational velocity, angular velocity and moment of inertia of the particle i, $\mathbf{R}_i$ a vector running from the centre of the particle to the contact point with its magnitude equal to particle radius R_i. $\mathbf{F}_{ij}^{\mathrm{n}}$ and $\mathbf{F}_{ij}^{\mathrm{s}}$ represent, respectively, the normal and the tangential contact forces imposed on particle i by particle j. Details about the force models can be found elsewhere [9,12,17].

The model IsaMill used in this work consists of a fixed chamber, a rotating shaft and three stirrers, as shown in Fig. 1. Initially the shaft and discs were at rest and all particles were fed into the mill to form a stable packed bed. Then the shaft and discs started to rotate at a given speed to agitate the particles. All simulations were carried out with the same rotation speed of 1000 rpm and the solid loading of 80%, but some particle properties were varied. Table 1 lists the base values and their varying ranges of the parameters used in the simulation. The effect of a parameter is examined while the others are fixed at their base values.

Table 1
Physical parameters used in the present simulation

Parameter	Base value	Varying range
Particle density, ρ (kg m^{-3})	2500	1000–7500
Young's modulus, Y (N m^{-2})	1.0×10^7	–
Poisson ratio, $\tilde{\sigma}$	0.29	–
Particle/particle sliding friction coefficient, $\mu_{\mathrm{s,pp}}$	0.2	0.01–1.0
Particle/mill sliding friction coefficient, $\mu_{\mathrm{s,pm}}$	0.2	–
Rolling friction coefficient, μ_{r}	0.01	–
Restitution coefficient, e	0.68	0.38–0.88
Particle diameter, d_{p} (mm)	3	2–4

3. Results and discussion

The validity of the numerical model has been examined elsewhere [12]. In this paper focus is given to the effects of particle material properties on the grinding performance. But whenever possible, numerical results will be compared with the experimental data and discussed in this section. The properties of particles considered in this work are particle/particle sliding friction coefficient $\mu_{\mathrm{s,pp}}$, particle restitution coefficient e, particle density ρ and particle diameter d_{p}. The particle flow is analysed in terms of flow velocity, local porosity, collision energy, collision frequency and power draw, which have been demonstrated to be useful to assess the performance of IsaMill [12]. Collision energy is defined as $1/2 m_i v_{ij}^2$, where m_i is the mass of a particle and $v_{ij}(= |\vec{v}_i - \vec{v}_j|)$ the magnitude of the relative velocity of two colliding particles. The spatial distributions of flow velocity and porosity are obtained, when the flow is macroscopically stable, by dividing the mill into a series of cells of 3 particle diameters in size and calculating the time averaged values for two complete revolutions for particles whose centres are located in the cell. All the analysis will be based on the particle flow in the central region of the model IsaMill as shown in Fig. 1, unless otherwise specified. In that case, the spatial variation is mainly observed in the radial direction. The so called statistical distribution of a property is calculated based on the data for the particles in the central region, collected within two revolutions of discs when the flow reaches its stable state.

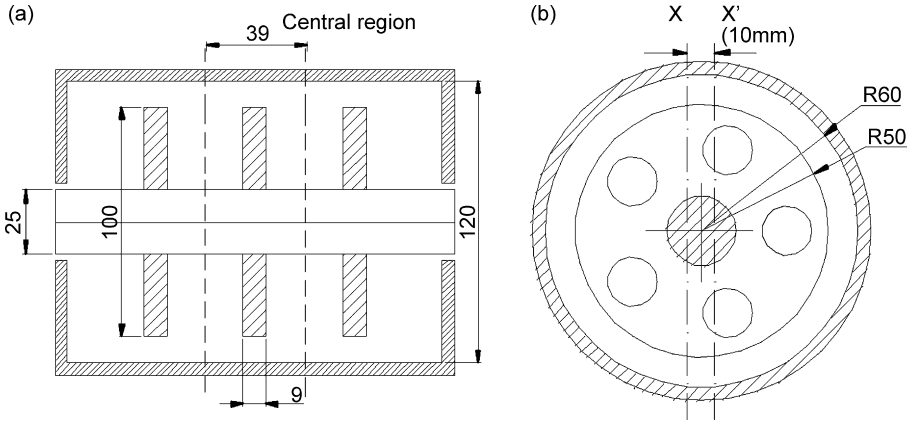

Fig. 1. Schematic illustration of the model IsaMill: (a) sectional front elevation and (b) sectional end elevation (all dimensions in mm).

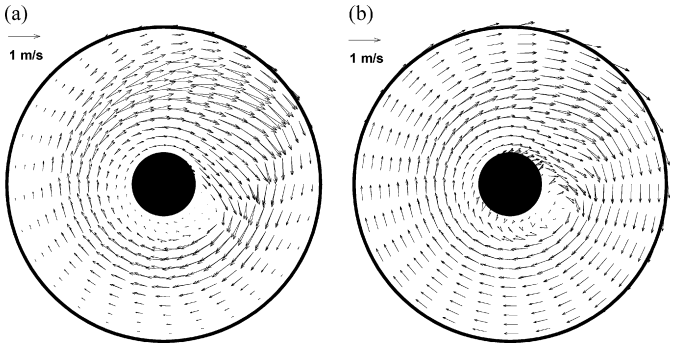

Fig. 2. Spatial distribution of velocities for different particle/particle sliding friction coefficients: (a) $\mu_{s,pp} = 0.01$ and (b) $\mu_{s,pp} = 1.0$.

3.1. Effect of sliding friction

Fig. 2 shows the flow velocity fields for different $\mu_{s,pp}$. For all the $\mu_{s,pp}$ considered, particles start to accelerate at 11 o'clock and collide with high velocity with the upper part of the drum. However, increasing $\mu_{s,pp}$ from 0.01 to 1.0 significantly reduces the velocity gradient in the radial direction. This is because, as sliding friction between particles increases, the energy transfer among particles becomes more efficient so the flow is strongly stratified, forming a moving bed around the chamber wall. This can also been seen from Fig. 3 which shows more homogeneous porosity distribution around the chamber wall for larger sliding friction coefficient. Note the high porosity at the upper part of mill for low sliding friction coefficient is due to the unconfined particle movement. As the grinding in IsaMill is mainly caused by the shear between layers of particles, the reduced velocity gradient will indeed decrease the grinding performance which is also reflected from the collision energy and collision frequency, as will be discussed below.

Figs. 4 and 5 show the distributions and the mean values of collision frequency C_f and collision energy C_e for different $\mu_{s,pp}$. While the collision frequency for low $\mu_{s,pp}$ has a wide distribution with a flat region from 300 to 500 Hz, the distribution becomes narrower with a sharp peak at less than 200 Hz as $\mu_{s,pp}$ increases. This leads to a sharp decrease in the mean collision frequency when $\mu_{s,pp}$ increases to 0.4. However, beyond this point the mean collision frequency is almost unchanged with only a slight increase. As mentioned above, the increase in $\mu_{s,pp}$ reduces the velocity gradient at radial direction so the particles move at a similar speed and behave like a solid bed. This reduces the chance of particles to collide with others. However, when $\mu_{s,pp}$ reaches to a critical point (0.4 for the system considered), further increase of $\mu_{s,pp}$ does not have effect on the collision frequency.

On the other hand, the mean collision energy has a peak value at around 0.2, as shown in Fig. 5b. Increasing $\mu_{s,pp}$ from 0.01 to 0.2 can lead to 30% increase in the collision energy. Considering 50% decrease in the collision frequency as shown in Fig. 4b, it is not very clear how the sliding friction affects the grinding efficiency. However, after $\mu_{s,pp} = 0.2$, increasing $\mu_{s,pp}$ decreases both the collision frequency and energy, which will reduce the grinding performance. These results are qualitatively in accordance with those reported by Xstrata Technology with the development of new grinding media called Keramax MT1 [2].

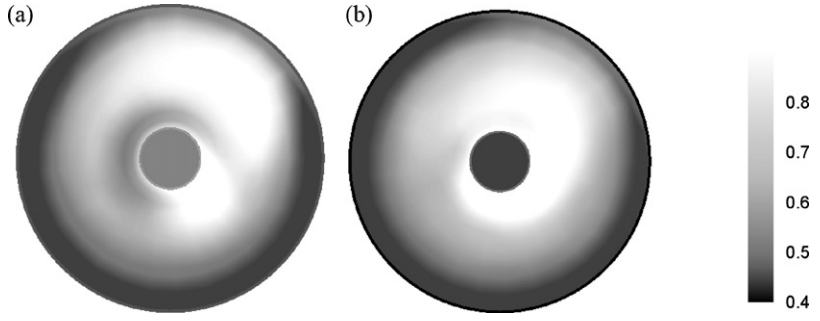

Fig. 3. Spatial distribution of porosity for different particle/particle sliding friction coefficients: (a) $\mu_{s,pp} = 0.01$ and (b) $\mu_{s,pp} = 1.0$.

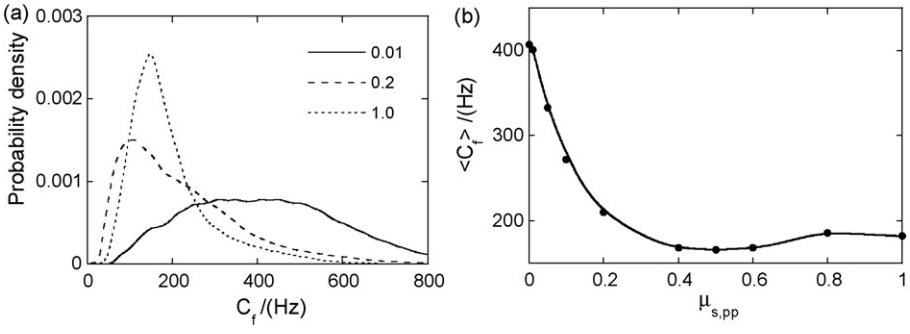

Fig. 4. Statistical distribution (a) and mean value (b) of the collision frequency for different particle/particle sliding friction coefficients.

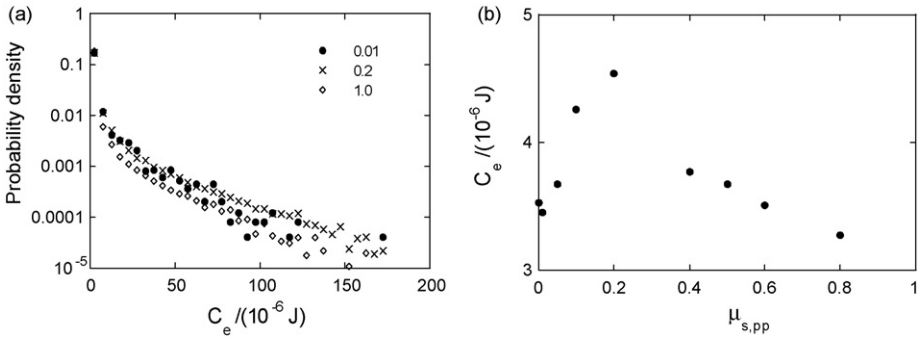

Fig. 5. Statistical distribution (a) and mean value (b) of the collision energy for different particle/particle sliding friction coefficients.

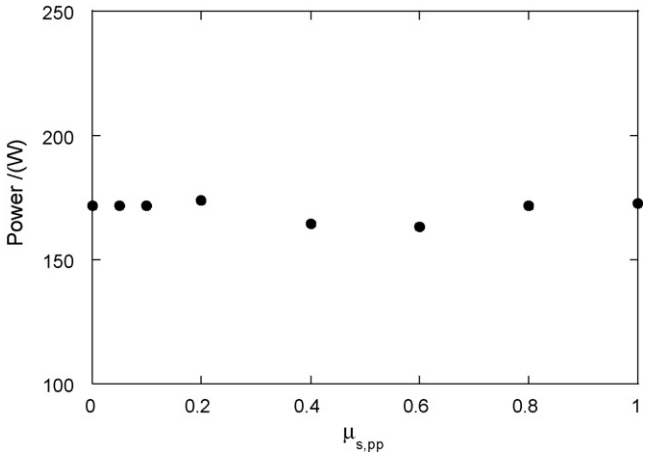

Fig. 6. Power draw as a function of particle/particle sliding friction coefficient.

Fig. 6 shows the variation of power draw with $\mu_{s,pp}$, indicating the sliding friction coefficient between particles has a negligible effect on the power draw. Note that, it was observed in our previous study of a single disc mill, the increase of both particle/particle and particle/mill sliding friction leads to an increase in power draw [13]. So the present results indicate that the increase in power draw is mainly caused by the increased particle/disk sliding friction.

3.2. Effect of restitution coefficient

Figs. 7 and 8 indicate that the restitution coefficient has a negligible effect on the velocity and porosity distributions. On the other hand, Figs. 9 and 10 show both collision energy and collision frequency increase with the restitution coefficient. A larger restitution coefficient means less energy dissipation

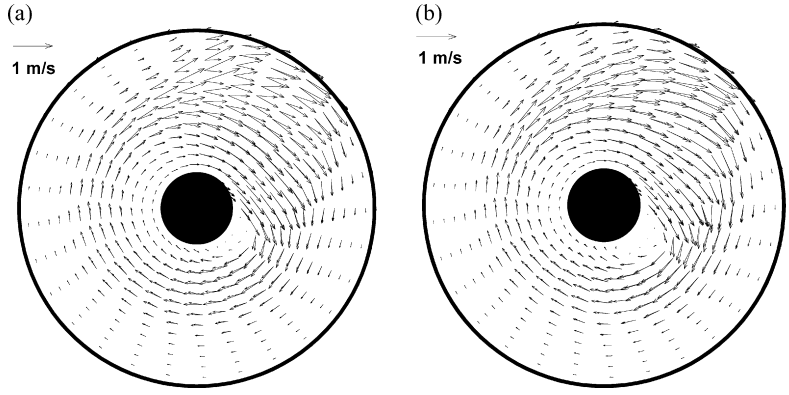

Fig. 7. Spatial distribution of velocities for different particle restitution coefficients: (a) 0.38 and (b) 0.88.

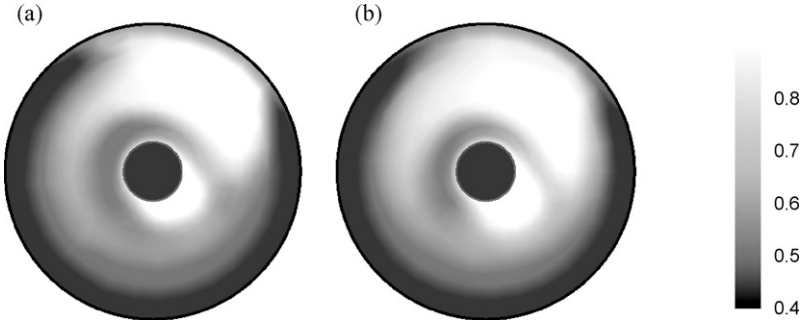

Fig. 8. Spatial distribution of porosity for different particle restitution coefficients: (a) 0.38 and (b) 0.88.

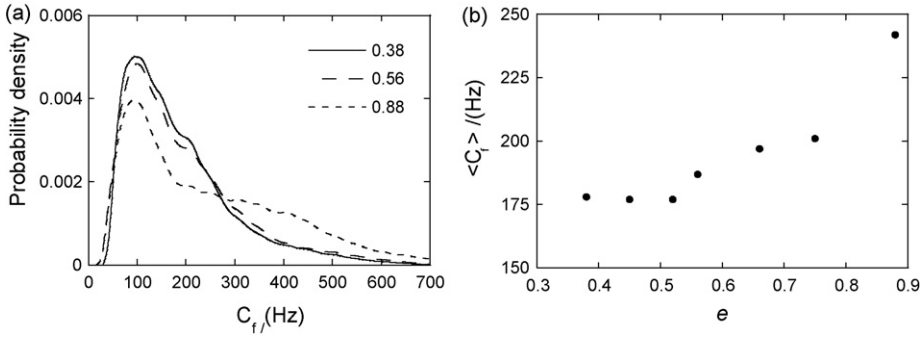

Fig. 9. Statistical distribution (a) and mean value (b) of the collision frequency for different restitution coefficients.

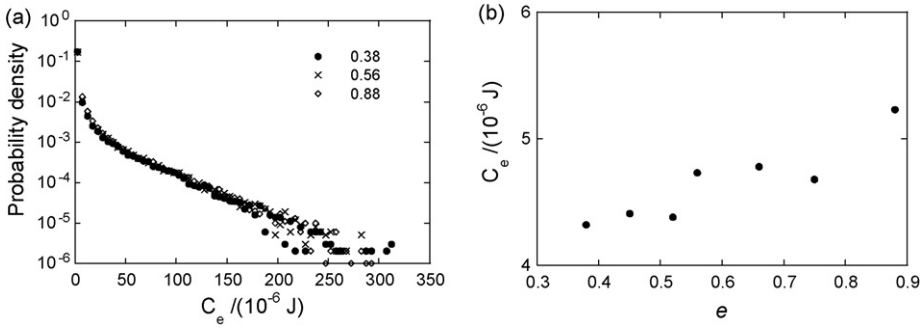

Fig. 10. Statistical distribution (a) and mean value (b) of the collision energy for different restitution coefficients.

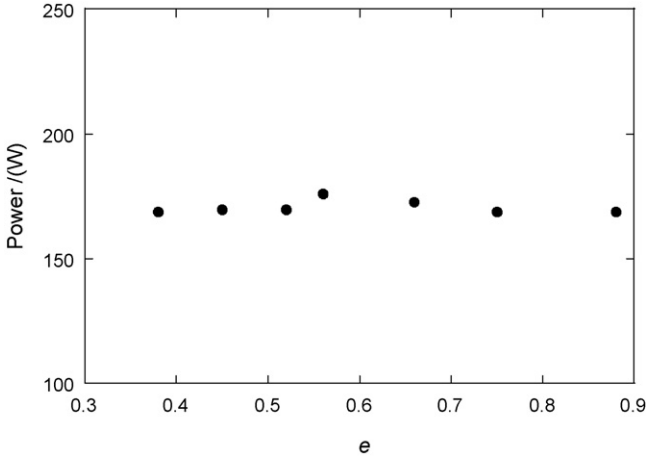

Fig. 11. Power draw as a function of restitution coefficient.

when particles collide, so particles move more vigorously leading to more collisions. Therefore, the collision frequency has a broader distribution and a larger mean $\langle C_f \rangle$ (Fig. 9). The same explanation is applicable to the collision energy (Fig. 10): less energy loss results in larger collision energy. The input power remains constant as the restitution coefficient increases, as shown in Fig. 11. For a large restitution coefficient, energy loss due to the dissipative collision becomes small, leading to high collision energy while maintaining a constant input power. Therefore, grinding media with high restitution coefficient can give better grinding performance than those with low restitution coefficient. Since materials with high hardness values tend to have high restitution coefficient, one may argue that grinding media with high hardness should be more effective than those with low hardness. This has been indeed observed in practice [2].

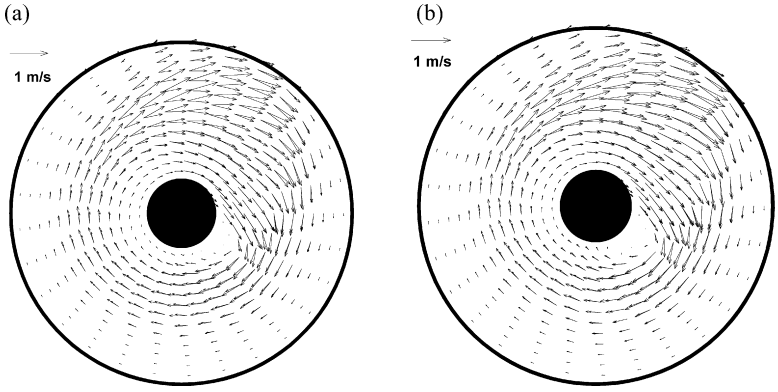

Fig. 12. Spatial distribution of velocities for different particle density: (a) $\rho = 1000\,\mathrm{kg\,m^{-3}}$ and (b) $\rho = 3500\,\mathrm{kg\,m^{-3}}$.

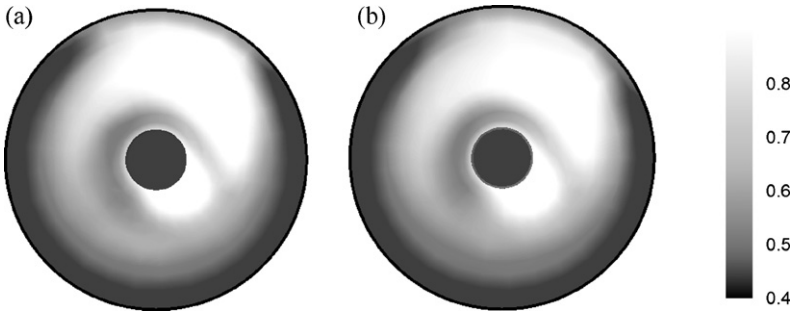

Fig. 13. Spatial distribution of porosity for different particle density: (a) $\rho = 1000\,\mathrm{kg\,m^{-3}}$ and (b) $\rho = 3500\,\mathrm{kg\,m^{-3}}$.

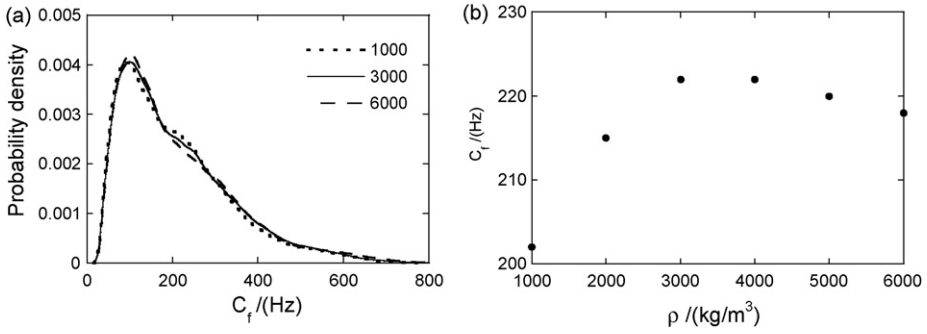

Fig. 14. Statistical distribution (a) and mean value (b) of the collision frequency for different particle density.

3.3. Effect of particle density

Figs. 12 and 13 show the spatial distributions of the flow velocity and porosity for different particle density ρ, which suggests that ρ has almost no significant effect, consistent with that reported elsewhere [14]. However, Figs. 14 and 15 show that both collision frequency and collision energy increases as particle density increases. It is understandable as the collision energy is directly proportional to the particle density and higher collision energy is expected for heavier particles. In conventional ball grinding, heavier grinding medium is always the first choice as long as it is practical. However, the results in Fig. 14b show that, for IsaMill process, the medium density has an optimum value at $\rho \approx 3000\,\mathrm{kg\,m^{-3}}$ which gives the highest collision frequency. These results are qualitatively in accordance with the results reported by Gao and Forssberg [18] with the Drais stirrer mill which is similar to IsaMill and has the similar dimensions with our numerical model. In his work the maximum energy utilisation was obtained at $3700\,\mathrm{kg\,m^{-3}}$ which is close to the ρ obtained here. Major part of the energy requirement for stirred milling involves stirring and lifting of the grinding media, energy required for lifting the media is directly associated with the particle density. Therefore, increase of ρ leads to increase in power consumption, as shown in Fig. 16.

To be more quantitative in model validation, physical experiments were conducted at different loading J and rotation speed Ω using two different particles: steel balls ($\rho = 7500\,\mathrm{kg\,m^{-3}}$) and glass beads ($\rho = 2500\,\mathrm{kg\,m^{-3}}$). The steel balls are assumed to have the same material properties as the glass beads as listed in Table 1, except for a slightly lower sliding coefficient of 0.18. Fig. 17 shows the power draw obtained from the experiments and simulations. Both numerical and experimental results showed that the power consumption for steel balls is higher than that for glass beads. For both materials, the experiment consistently produces slightly a higher power draw than the simulation. This has also been observed in our previous work [12]. The discrepancy

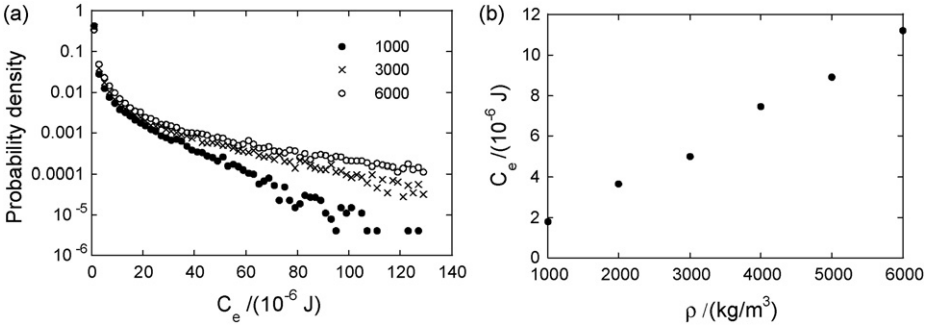

Fig. 15. Statistical distribution (a) and mean value (b) of the collision energy for different particle densities.

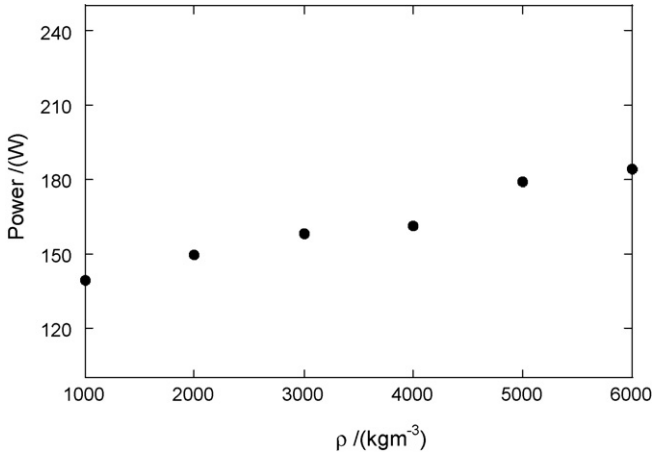

Fig. 16. Power draw as a function of particle density.

at high rotation speeds can be attributed to the mechanical and other energy losses (e.g. sound and heat) which are not considered in the simulation. Nevertheless, the trends between the numerical and physical results are quite comparable.

3.4. Effect of particle size

The size of the grinding medium is one of the most significant factors which affect the mill performance [15]. To understand the effect of medium size, we have varied the particle size from 2 to 5 mm. Figs. 18 and 19 show the representative flows from simulations and experiments for different solid loadings and rotation speeds for 5 mm particles. It can be seen that the overall flow patterns obtained from the experiments and simulations are comparable. At low solid loading and low rotation speed (Figs. 18a and 19a), most of particles stay at the bottom of the mill with slow movement, and only a small number of particles are agitated by the rotating disc to the upper half of the mill. Increasing either the solid loading or the rotation speed (Figs. 18b and 19b) can agitate the particles more vigorously due to the increased collisions between particles and between particles and disc.

Fig. 20 shows experimental and numerical power draw for 3 mm and 5 mm particles. It can be seen that for both particle sizes, power draw increases with rotation speed. The overall results from simulation and experiments are quite comparable, and the discrepancy at high rotation speeds can also be attributed to the mechanical and other energy losses as discussed above. The good agreement observed further confirms the validity of the proposed numerical approach in the study of particle flow in IsaMill.

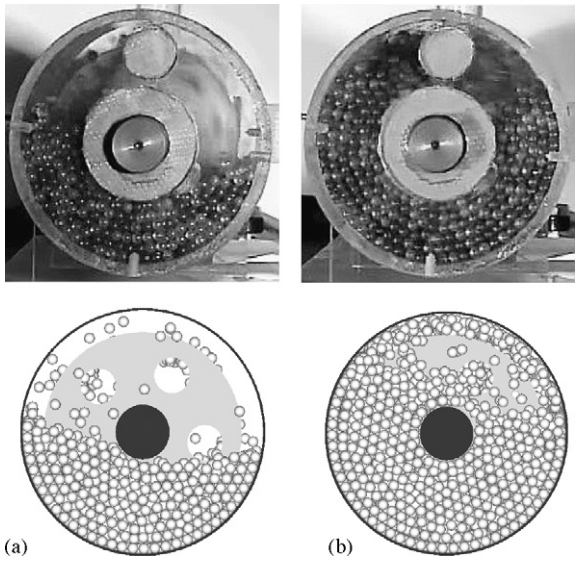

Fig. 18. End view of experimental (top) and numerical (bottom) particle distributions for different solid loadings and rotation speeds for glass beads: (a) $\Omega = 300$ rpm and $J = 40\%$; (b) $\Omega = 800$ rpm and $J = 60\%$.

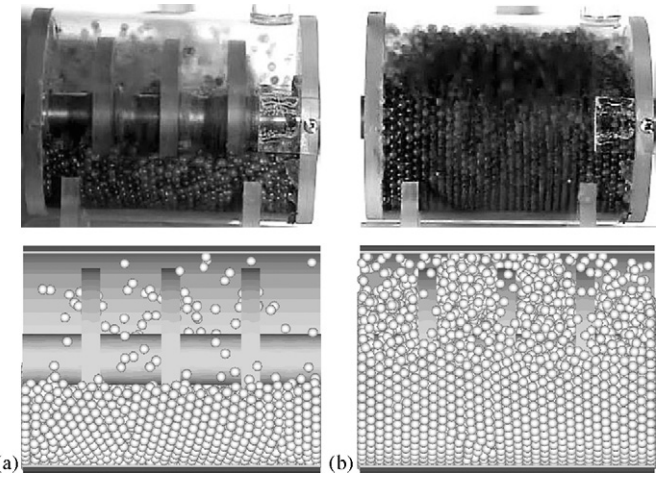

Fig. 19. Axial view of experimental (top) and numerical (bottom) particle distributions for different solid loadings and rotation speeds for glass beads:(a) $\Omega = 300$ rpm and $J = 40\%$; (b) $\Omega = 300$ rpm and $J = 60\%$.

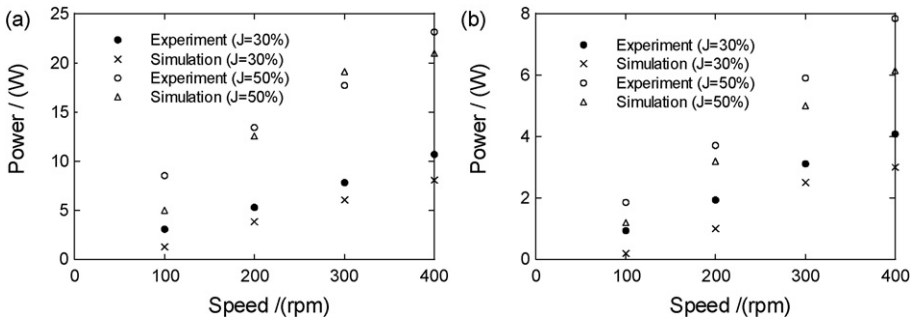

Fig. 17. Power comparison between physical experiments and numerical simulations for (a), steel balls and (b), glass beads at different loadings and rotation speeds.

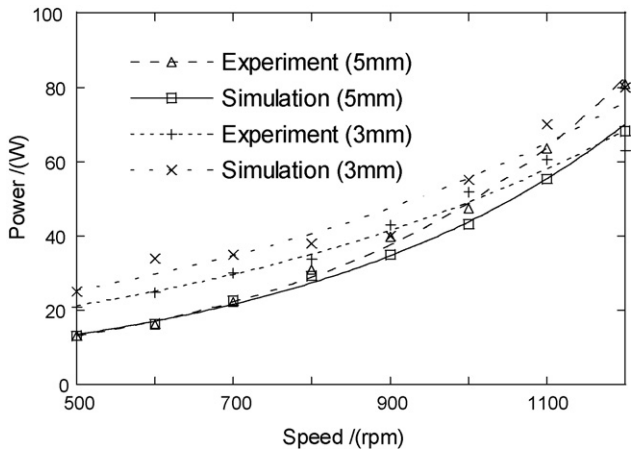

Fig. 20. Experimental and numerical power draw comparison for 3 mm and 5 mm particles.

Figs. 21 and 22 show that 2 mm particle flow has quite inhomogeneous distribution of velocity and porosity in the radial direction, and in contrast, the flow of 4 mm particles shows quite uniform distributions. 2 mm particles in the mill obtain high velocities at 11 o'clock and then accelerate to collide with the upper part of the drum, leading to a high porosity zone between 11 and 2 o'clock. On the other hand, 4 mm particles give a reduced velocity gradient along the radial direction. Particles with high velocities tend to move towards the mill chamber, creating a large porosity zone in the middle near the shaft.

The velocity and porosity distributions in the axial direction also reveal interesting differences for the two sized particles, as shown in Fig. 23. 2 mm particles have a small circulating flow, caused by the centrifugal effect generated by the rotating discs. In order to satisfy the continuity condition, particles have to flow

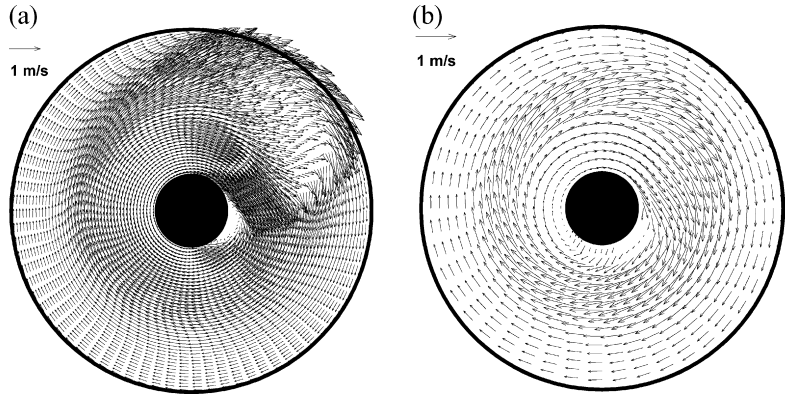

Fig. 21. Spatial distribution of velocities for different particle sizes: (a) $d_p = 2$ mm and (b) $d_p = 4$ mm.

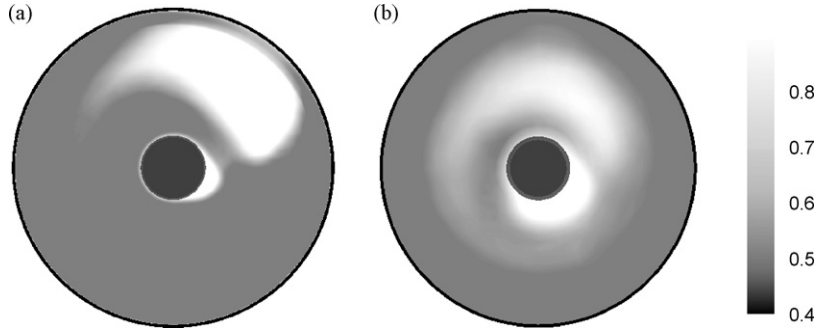

Fig. 22. Spatial distribution of porosity for different particle sizes: (a) $d_p = 2$ mm and (b) $d_p = 4$ mm.

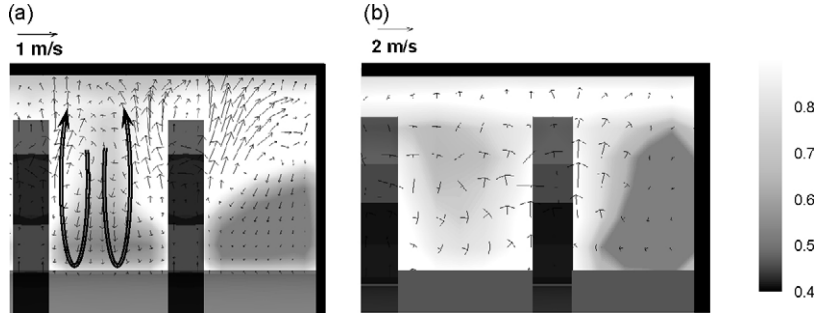

Fig. 23. Spatial distribution of velocity and porosity for different particle sizes in the upper region of sectional elevation at XX': (a) $d_p = 2$ mm and (b) $d_p = 4$ mm.

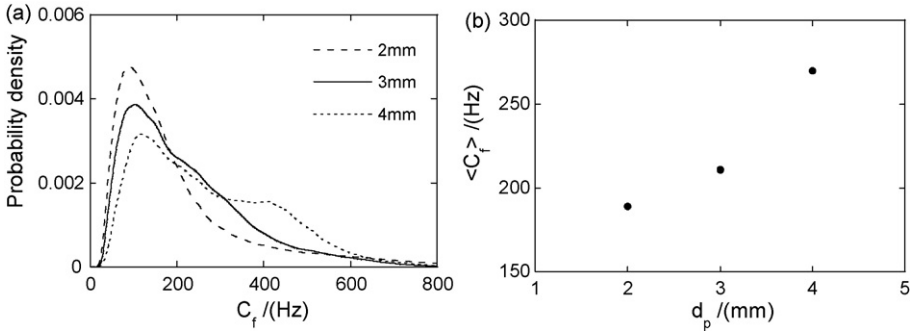

Fig. 24. Statistical distribution (a) and mean value (b) of the collision frequency for different particle sizes.

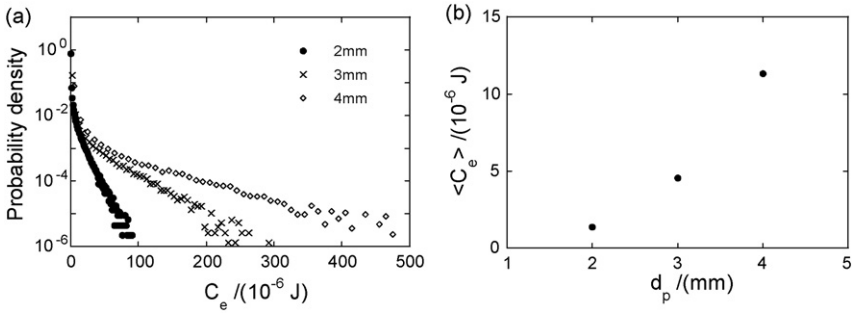

Fig. 25. Statistical distribution (a) and mean value (b) of the collision energy for different particle sizes.

back to the shaft from where it is driven outward again. In the vicinity of the discs, particles obtain high velocities; while in the regions near the shaft, particles have low velocities profile. When particle size is increased to 4 mm, circulatory flow in the axial direction diminishes (Fig. 23b) due to the same effect, but less distinct velocity profile. High porosity regions are evident in between discs and low porosity regions develop close to the end wall.

Figs. 24 and 25 show the collision frequency and collision energy for different particle sizes, indicating both the collision frequency and the collision energy increase with increasing particle size. The number of particles decreases about 8 times (from 117,000 to 14,400) to keep the same 80% solid loading when particle size increases from 2 to 4 mm. The 50% increase in the collision frequency means that the total number of collisions for 2 mm particles is still 5 times that of 4 mm particles. On the other hand, the collision energy has 5 times increase when particle size increases from 2 to 4 mm. The decreased number of collision and increased collision energy form two competitive mechanisms when assessing grinding performance. It suggests there may exist an optimum grinding medium size which gives a good balance of the collision number and energy. This optimum size may vary with milling systems and depend on the size of the product. For a stirred mill, the most efficient grinding was obtained with 1.7–1.2 mm media [19].

The decrease of the power draw with particle size (Fig. 26) can be attributed to the reduced number of collisions between particles. As energy is dissipated from each collision, less collision between particles requires less input energy to maintain the flow dynamics. As discussed earlier, the simulated power draw agrees reasonably well with the measured one (Fig. 20).

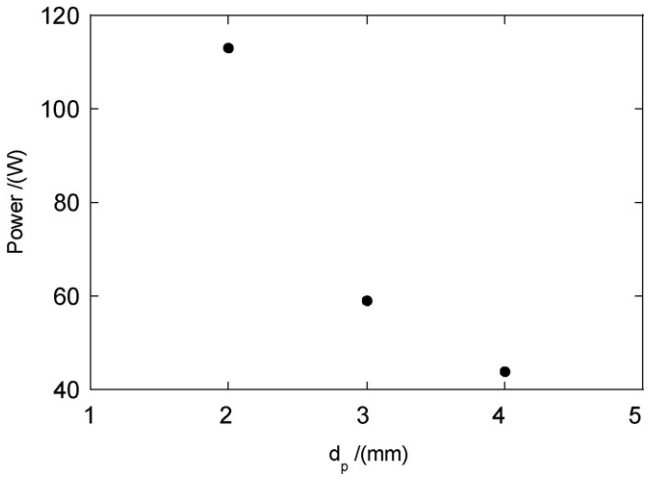

Fig. 26. Power draw as a function of particle size.

4. Conclusions

DEM has been employed to investigate the effects of grinding medium properties on the particle flow and grinding performance in a simplified IsaMill. The properties considered include particle/particle sliding friction coefficient, restitution coefficient, particle density and particle size and the flow properties. Their effects are examined in terms of flow velocity, porosity, collision energy, collision frequency and power draw. The results can be summarized as:

- Increasing particle/particle sliding friction decreases the velocity gradient in the radial direction. When the sliding fric-

tion coefficient is smaller than a critical value, increasing the sliding friction coefficient decreases the collision frequency and increases the collision energy. When the friction coefficient is higher than the critical value, increasing the sliding friction coefficient decreases both the collision frequency and the collision energy, and hence the grinding performance. Power draw is not sensitive to the friction.

- For the range considered, particle/particle restitution coefficient has little effect on the velocity and porosity distributions, and power draw as well. But a high restitution coefficient can result in a high collision frequency and collision energy, which is beneficial to grinding.
- Particle density does not evidently affect the velocity and porosity distributions. However, heavier particles have a high number of collisions and collision energy, and need a high power input. For a given IsaMill process, there may exist an optimum particle density for maximum process efficiency.
- Smaller particles have a larger number of collisions for given operational conditions (e.g. constant solid loading), although the number of collision for each particle is lower. On the other hand, larger particles have larger collision energy. The two competitive mechanisms suggest that there may exist an optimum particle size for better grinding. But this optimum size is also dependent on the size of the ground products. The power draw decreases with the increase of particle size.

Acknowledgements

The authors would like to thank the Australian Research Council and Xstrata Technology for providing the financial support for this work. The permission granted by Xstrata Technology to publish this paper is gratefully acknowledged.

References

[1] M. Gao, M.F. Young, B. Cronin, G. Harbort, IsaMill medium competency and its effect on milling performance, Miner. Metall. Process. 18 (2001) 117–121.
[2] D.C. Curry, B. Clermont, Improving the efficiency of fine grinding—development in ceramic media technology, in: Randol Innovative Metallurgy Conference, Perth, Australia, 2005.
[3] M.W. Gao, E. Forssberg, Prediction of product size distributions for a stirred ball mill, Powder Technol. 84 (1995) 101–106.
[4] G.L. Lane, CFD modelling of a stirred bead mill for fine grinding, in: Second International Conference on CFD in the Minerals and Process Industries, Melbourne, Australia, 1999.
[5] P.A. Cundall, O.D.L. Stack, A discrete numerical model for granular assemblies, Geotechnique 29 (1979) 47–52.
[6] J. Kano, F. Saito, Correlation of powder characteristics of talc during planetary ball milling with the impact energy of the balls simulated by the particle element method, Powder Technol. 98 (1998) 166–170.
[7] P.A. Langston, U. Tuzun, D.M. Heyes, Discrete element simulation in granular flow in 2D and 3D Hoppers: dependence of discharge rate and wall stress on particle interactions, Chem. Eng. Sci. (1995) 967–987.
[8] B.K. Mishra, A review of computer simulation of tumbling mills by the discrete element method Part II—practical applications, Miner. Process. 71 (2003) 95–112.
[9] R.Y. Yang, R.P. Zou, A.B. Yu, Microdynamic analysis of particle flow in a horizontal rotating drum, Powder Technol. 130 (2003) 138–146.
[10] P.W. Cleary, Recent advance in DEM modelling of tumbling mills, Miner. Eng. 14 (2001) 1295–1319.
[11] D.I. Hoyer, The discrete element method for fine grinding scale-up in Hicom mills, Powder Technol. 105 (1999) 250–256.
[12] C.T. Jayasundara, R.Y. Yang, A.B. Yu, D. Curry, Discrete particle simulation of particle flow in IsaMill, Ind. Eng. Chem. Res. 45 (2006) 6349–6359.
[13] R.Y. Yang, C.T. Jayasundara, A.B. Yu, D. Curry, DEM simulation of the flow of grinding medium in IsaMill, Miner. Eng. 19 (2006) 984–994.
[14] C.T. Jayasundara, R.Y. Yang, A.B. Yu, D. Curry, Discrete particle simulation of particle flow in IsaMill—effect of mill properties, in: Comminution 06, Perth, Australia, 2006.
[15] P. Wolfgang, Materials properties in fine grinding, Int. J. Miner. Process. 74S (2004) 3–17.
[16] H. Rumpf, Physical aspects of comminution and new formulation of a law of comminution, Powder Technol. 7 (1973) 145–159.
[17] R.Y. Yang, R.P. Zou, A.B. Yu, Computer simulation of packing of fine particles, Phys. Rev. E 62 (2000) 3900–3908.
[18] M.-W. Gao, E. Forssberg, A study on the effect of parameters in stirred ball milling, Int. J. Miner. Process. 37 (1992) 45–49.
[19] A. Jankovic, Variables affecting the fine grinding of minerals using stirred mills, Miner. Eng. 16 (2003) 337–345.